PUBLIC HEALTH

Identifying heat-related diagnoses in emergency department visits among adults in Chicago: A heat-wide association study

Hyojung Jang[1]*, Peter M. Graffy[1,2]†, Benjamin W. Barrett[1,2]†, Daniel E. Horton[2,3], Jennifer L. Chan[2,4], Abel N. Kho[1,2,5]

Extreme heat is an escalating public health concern. Although prior studies have examined heat-health associations, their reliance on restricted diagnoses and diagnostic categories may miss or misclassify heat-related illness. Here, we conducted a heat-wide association study to evaluate acute-care diagnoses associated with extreme heat in Chicago, Illinois. Using 916,904 acute-care visits—including emergency department and urgent care encounters—among 372,140 adults across four health care systems from 2011 to 2023, we applied a two-stage analytic approach: quasi-Poisson regression to screen diagnosis codes associated with heat, followed by distributed lag nonlinear models in a time-stratified case-crossover design to characterize exposure-response and lag patterns. Stage 1 retained 44 diagnosis codes, and 33 clinically reportable diagnoses were retained after stage 2. We observed elevated cumulative odds over lags 0 to 3 for multiple diagnoses, including fluid-balance and renal disorders, dermatologic and pressure-related conditions, multiple sclerosis, a cannabinoid-related mental and behavioral disorder, varicose veins of the lower extremities, and multiple injuries and external causes. By analyzing the full diagnostic spectrum of acute-care services, this study improves the clinical characterization of heat-associated morbidity in acute-care settings.

INTRODUCTION

Extreme heat exposure is an escalating public health concern, with climate change driving increases in the frequency, intensity, and duration of heat events (*1*, *2*). Both the frequency and duration of heat events have increased substantially since the 1950s, with nearly one-third of the global population now experiencing at least 20 days of extreme heat annually (*3*, *4*). Alongside this global trend, urban environments face additional risks because of the urban heat island effect, which can elevate local temperatures by several degrees and prolong heat events (*5*, *6*).

Extreme heat places a substantial strain on health systems, prompting extensive study of its effects on morbidity, mortality, and health care utilization. Studies have demonstrated that extreme heat is associated with increased all-cause mortality (*7*–*15*) and heat-specific illnesses such as heat exhaustion and heat stroke (*16*–*18*). Morbidity also rises during extreme heat, including cardiovascular and respiratory events (*19*–*22*), renal disease and electrolyte disturbances including hyponatremia (*19*, *23*–*26*), worsening mental health outcomes (*27*, *28*), and increased injury incidence (*7*, *29*). Consistent with these clinical impacts, health care use increases, with surges in emergency department (ED) visits and hospital admissions (*16*–*19*, *22*–*25*, *30*–*35*).

Despite these advances in our understanding of the health effects of extreme heat, many studies have taken a deductive, hypothesis-driven approach with preselected diagnoses and diagnostic categories to define heat-related illness, yielding valuable but potentially incomplete coverage of heat-related morbidity. Furthermore, heat-related health outcomes are difficult to define because of their diverse symptom presentation leading to nonspecific documentation of conditions or diagnoses and undercategorization of clinical conditions as explicitly “heat-related”—especially in emergency settings (*36*). These challenges complicate studies on heat-associated morbidity and can lead to underestimation of the true public health impact of extreme heat. Moreover, such underestimation may obscure the disproportionate impacts experienced by socially and economically vulnerable populations, who often have limited adaptive capacity and face greater risks from extreme heat (*37*–*39*). Addressing this knowledge gap is critical to more completely capture the full extent of heat-related health risks, which can inform preparedness strategies and support equitable public health interventions.

Here, we apply a “heat-wide association study” (HWAS)—an inductive, data-driven framework to systematically evaluate the short-term impact of extreme heat across the full spectrum of International Classification of Disease (ICD)–coded diagnoses in ED and urgent care (UC) visits within a large integrated urban health care network in Chicago, Illinois. Chicago—marked by high-density development, a pronounced urban heat island, and a documented history of heat-related morbidity and mortality—provides the sociodemographic diversity and health care infrastructure needed to study acute care–based heat risks at the city level (*9*, *33*, *40*, *41*). The Chicago Area Patient-Centered Outcomes Research Network (CAPriCORN) (*42*) links electronic health record (EHR) data from multiple Chicago-based health care systems, representing a sociodemographically and geographically diverse urban patient population. Patient residential data in CAPriCORN enable spatial linkage of environmental exposures to clinical outcomes, providing a robust platform for studying conditions with increased acute-care visit risk during extreme heat events (*43*).

Our analysis used retrospective acute-care encounters—ED and UC visits—from four health care systems in CAPriCORN. Throughout

[1]Division of Biostatistics & Informatics, Department of Preventive Medicine, Feinberg School of Medicine, Northwestern University, Chicago, IL 60611, USA. [2]Defusing Disaster Working Group, Buffett Institute for Global Affairs, Northwestern University, Evanston, IL 60208, USA. [3]Department of Earth, Environmental, and Planetary Sciences, Northwestern University, Evanston, IL 60208, USA. [4]Department of Emergency Medicine, Feinberg School of Medicine, Northwestern University, Chicago, IL 60611, USA. [5]Department of Medicine, Feinberg School of Medicine, Northwestern University, Chicago, IL 60611, USA.
*Corresponding author. Email: hyojung.jang@northwestern.edu
†These authors contributed equally to this work.

this manuscript, we use ED as a shorthand, representing both ED and UC visits, collectively referred to as acute-care services. The analytic cohort comprised 916,904 ED visits among 372,140 unique adult (≥18 years) patients during the warm season (May to September) from 2011 through 2023. We examined all 1803 distinct ICD-10 and ICD-9 equivalent diagnosis categories, as captured in CAPriCORN ED visits, as outcomes of interest. We standardized ICD-9 codes to their corresponding ICD-10 categories for consistency (see Materials and Methods). Multi-institution EHR data require attention to temporal variation in site coverage, coding practices, and patient case mix. Accordingly, we first examined temporal patterns in data composition and case mix across the analytic cohort before conducting diagnosis-specific association modeling.

We then implemented a two-stage analytic framework—quasi-Poisson screening followed by time-stratified case-crossover distributed lag nonlinear models (DLNMs)—to manage the high-dimensional diagnosis space in a structured way. The first stage served as an exploratory screening step to select diagnosis categories for follow-up analysis, whereas the second stage was used to characterize the exposure-response and lag patterns of selected diagnosis categories in relation to extreme heat. Figure 1 describes the overall analytic approach. In the first stage, we fit diagnosis-specific quasi-Poisson regressions of daily ED visit counts on the 3-day moving average of daily maximum temperature as an exploratory screening step to prioritize codes whose counts increased on hotter days, adjusting for long-term and seasonal time trends of calendar time, day of week, holidays, and same-day Cook County mean particulate matter with a diameter of 2.5 μm or less ($PM_{2.5}$) derived from Environmental Protection Agency (EPA) monitors (*44*) and controlling the false discovery rate (FDR) with Benjamini-Hochberg (BH) adjustment (*45*). In the second stage, we fit DLNMs in a time-stratified case-crossover design (*13*, *46*), adjusted for the same daily $PM_{2.5}$ measure, to estimate short-term cumulative associations between extreme heat and the diagnosis codes retained from stage 1. The two-stage analysis was designed to manage a high-dimensional diagnosis space by using stage 1 for structured outcome screening and stage 2 for more detailed characterization of the retained diagnoses.

The two stages serve different analytic roles and operate at different levels of analysis. Stage 1 is an aggregate-level ecological screening step: Quasi-Poisson models of daily citywide counts identify diagnosis codes whose population-level visit volumes are sensitive to ambient temperature but cannot control for individual-level confounders, cannot characterize nonlinear exposure-response relationships, and cannot model distributed lag effects. Stage 2 adds individual-level characterization: The time-stratified case-crossover design controls for time-invariant individual-level confounders through within-person matching, and the DLNM cross-basis captures both the nonlinear exposure-response and lag structure at the individual level. Stage 1 is therefore used as a dimension reduction filter to make the individual-level stage 2 analysis computationally tractable across 1803 codes, rather than as a source of inference itself.

We then stratified analyses by demographic and neighborhood characteristics to describe subgroup patterns in heat vulnerability. We also conducted sensitivity analyses to evaluate the robustness of our model specifications and findings. Leveraging more than a decade of multi-institutional EHR data linked to high-resolution temperature data, this study provides a broad descriptive and analytic assessment of diagnosis-specific acute-care utilization in relation to extreme heat at a citywide scale. This approach not only enables the systematic evaluation of underrecognized heat-sensitive conditions

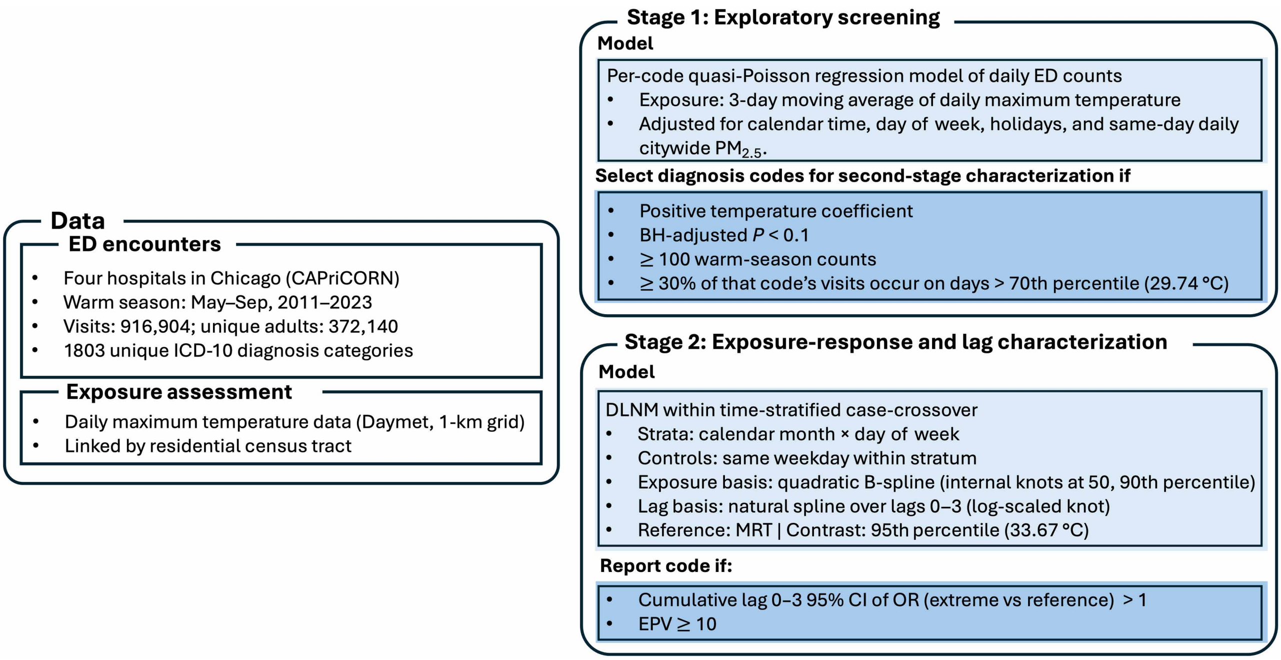

Fig. 1. Two-stage analytic workflow. Stage 1 screened 1803 ICD-10 diagnosis categories using diagnosis-specific quasi-Poisson models of daily ED/UC counts and the 3-day moving average of daily maximum temperature, adjusting for calendar time, day of week, holidays, and same-day Cook County EPA monitor–based daily $PM_{2.5}$. Codes with a positive temperature coefficient, BH-adjusted $P < 0.10$, at least 100 warm-season counts, and at least 30% of visits on days above the 70th temperature percentile were retained. Stage 2 used time-stratified case-crossover DLNMs over lags 0 to 3 and adjusted for the same daily $PM_{2.5}$ measure. Stage 2 reporting required a cumulative lag 0-to-3 lower 95% CI >1 and EPV ≥10.

but also facilitates subgroup analyses to describe heat-related health outcome patterns across demographic and neighborhood contexts (see Materials and Methods for analytic details).

RESULTS

Study population and heat exposure summary

Among 372,140 adults with ED visits, females accounted for 57.9% of patients, and the mean age of patients was 52 years (standard deviation, 19.4 years). Table 1 summarizes patient demographics across ED visits and the geographic distributions of residences by heat exposure category. Over the study period, there were 100 extreme heat days [≥33.67°C (92.60°F); 95th percentile of daily maximum temperature during the warm season] and 1882 nonextreme heat days. Extreme heat days were concentrated in mid-summer, occurring most frequently in July (36%), followed by August (25%), June (23%), September (12%), and May (4%). When stratified by year, the highest frequency of extreme heat days was observed in 2012 (25%), followed by 2018 (15%) and 2011 (13%). Demographic and geographic distributions were broadly similar between nonextreme heat and extreme heat days, indicating comparable patient profiles across exposure categories. Adults aged 25 to 44 years represented the largest age group, Black or African American patients comprised the majority by race/ethnicity, and the West Side of Chicago contributed the highest share of ED visits.

Within the warm-season analytic cohort, temporal patterns varied across calendar years in visit volume, contributing-site composition, patient characteristics, and diagnostic composition. Annual acute-care visit volume and the number of unique patients increased during the early study period and generally declined thereafter, with corresponding variation in average annual number of visits per unique patient (fig. S1). The relative contribution of participating health care systems also changed over time, indicating that the analytic cohort was not compositionally static across the calendar year (fig. S2). Patient composition varied modestly over time. The share of visits among adults aged 65 years or older increased, whereas the share among adults aged 18 to 24 and 25 to 44 years declined modestly; sex composition remained relatively stable, and racial and ethnic

Table 1. Cohort characteristics by heat exposure category. Characteristics of patients across ED/UC visits by heat exposure category during warm-season months (May to September), 2011 to 2023. Nonextreme heat days are dates with daily maximum temperature <95th percentile; extreme heat days are ≥95th percentile of the warm-season daily maximum temperature distribution. Age (18 to 24, 25 to 44, 45 to 64, and ≥65 years), sex (female, male, and other), and race/ethnicity (Asian, Black or African American, white, and other) are reported as recorded in the EHR; "missing" reflects unavailable data. The geographic region corresponds to Chicago community regions (Central, North, Northwest, South, Southwest, Far South, and West Side), assigned using residential census tract centroids.

	Nonextreme heat days (*N* = 884,662)	Extreme heat days (*N* = 32,242)	Total (*N* = 916,904)
Age (years)			
18–24	90,496 (10.2%)	3,541 (11.0%)	94,037 (10.3%)
25–44	335,891 (38.0%)	12,404 (38.5%)	348,295 (38.0%)
45–64	257,275 (29.1%)	9,276 (28.8%)	266,441 (29.1%)
65+	156,279 (17.7%)	5,433 (16.9%)	161,712 (17.6%)
Missing	44,721 (5.1%)	1,588 (4.9%)	46,309 (5.1%)
Sex			
Female	511,695 (57.8%)	18,683 (57.9%)	530,378 (57.8%)
Male	372,804 (42.1%)	13,553 (42.0%)	386,357 (42.1%)
Other	60 (0.0%)	2 (0.0%)	62 (0.0%)
Missing	103 (0.0%)	4 (0.0%)	107 (0.0%)
Race/ethnicity			
Asian	15,945 (1.8%)	577 (1.8%)	16,522 (1.8%)
Black or African American	472,467 (53.4%)	17,655 (54.8%)	490,122 (53.5%)
White	244,368 (27.6%)	8,984 (27.9%)	253,352 (27.6%)
Other	114,822 (13.0%)	3,699 (11.5%)	118,521 (12.9%)
Missing	37,060 (4.2%)	1,327 (4.1%)	38,387 (4.2%)
Region of Chicago			
Central Side	92,968 (10.5%)	3,077 (9.5%)	96,045 (10.5%)
Far South Side	55,316 (6.3%)	1,895 (5.9%)	57,211 (6.2%)
North Side	85,679 (9.7%)	2,971 (9.2%)	88,650 (9.7%)
Northwest Side	74,368 (8.4%)	2,618 (8.1%)	76,986 (8.4%)
South Side	101,818 (11.5%)	3,666 (11.4%)	105,484 (11.5%)
Southwest Side	118,012 (13.3%)	4,593 (14.2%)	122,605 (13.4%)
West Side	275,639 (31.2%)	10,546 (32.7%)	286,185 (31.2%)
Missing	80,862 (9.1%)	2,876 (8.9%)	83,738 (9.1%)

composition shifted modestly across years (fig. S3). Diagnostic composition also changed over time. The relative distribution of major diagnosis chapters varied across calendar years, indicating that the clinical profile of acute-care utilization was not static over the study period (fig. S4). In particular, R-coded (symptom- and sign-based) diagnoses represented an increasing share of diagnosis records overall, with additional variation across participating health care systems (fig. S5). These temporal trends in cohort composition are documented and presented in figs. S1 to S5 to support transparent assessment of potential data quality influences on our primary findings.

Visit frequency was right-skewed: 10.7% of patients (n = 39,763 with ≥5 summer ED visits over 2011 to 2023) contributed 45.1% of all summer ED encounters. Among patients with race recorded, frequent users were more likely to identify as Black or African American (66.3% versus 42.2%), and they were also more often female (62.3% versus 55.3%).

Compared with the Chicago adult population using period-matched Census references, the EHR cohort was broadly representative by age and sex and divergent in racial/ethnic and geographic composition; full domain-specific comparisons are shown in fig. S6. The period-averaged Census reference was stable over the study period, while the EHR cohort underwent demographic shifts—the 65+-year share rose by 10.6 percentage points and the Black patient share declined by 9.6 percentage points from 2011 to 2023.

First-stage screening analysis of diagnosis codes

The stage 1 screening procedure retained 44 diagnosis codes meeting all prespecified screening criteria: a positive temperature coefficient, BH-adjusted $P < 0.10$, at least 30% of visits occurring on days above the warm-season 70th temperature percentile (29.74°C), and at least 100 warm-season counts. Figure 2 shows the first-stage screening results in a Manhattan plot. Each point represents an individual diagnosis code, with the vertical axis showing $-\log_{10}$ of the BH-adjusted P value from the diagnosis-specific quasi-Poisson models. The dashed red line marks the prespecified stage 1 screening threshold of BH-adjusted $P = 0.1$. Labels identify codes that also met the frequency criteria [≥30% of ED visits on days above the 70th temperature percentile (29.74°C) and ≥100 counts of diagnosis code]. A complete listing of the selected diagnoses, including ICD-10 descriptions, chapters, incidence rate ratios, BH-adjusted P values, and the proportion of visits occurring on days above the 70th percentile of the temperature distribution, is provided in table S1. These frequency-based criteria were intended to support stable candidate diagnosis prioritization in a high-dimensional screening setting, rather than to define clinically meaningful cut points.

Second-stage lag-specific and cumulative effects of extreme heat

The first-stage quasi-Poisson screening served as a dimension-reduction step, retaining 44 of 1803 diagnosis categories. In the second stage, we characterized the complete exposure-response relationship for each of these candidate diagnoses using DLNMs within a time-stratified case-crossover design, estimating both immediate and short-term temperature effects. The exposure contrast compared the warm-season 95th-percentile daily maximum temperature [33.67°C (92.60°F)] with the diagnosis-specific minimum risk temperature

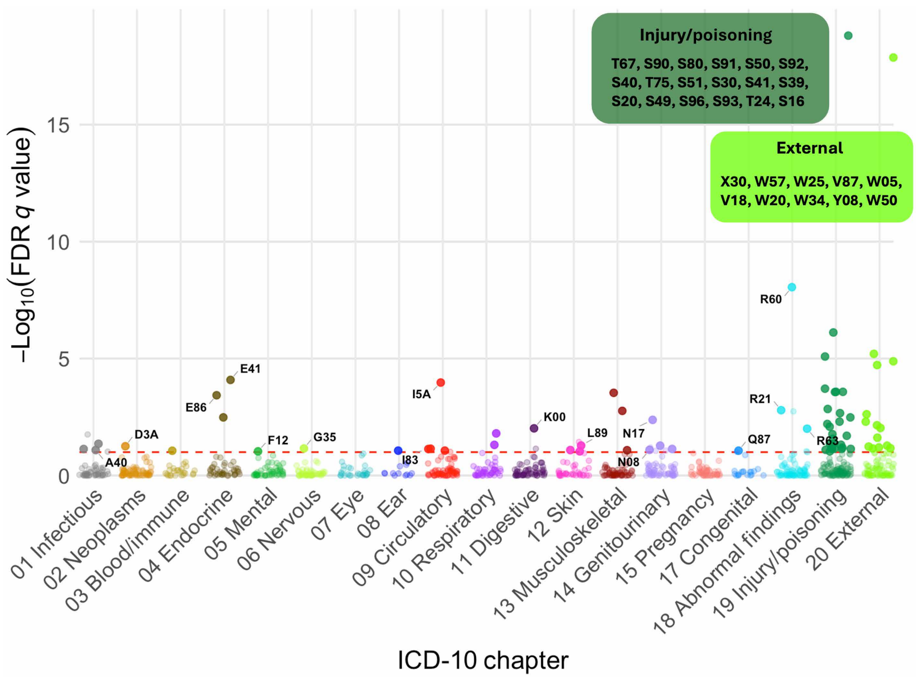

Fig. 2. Stage 1 screening results across 1803 diagnosis categories. Each point represents an ICD-10 diagnosis code; the y axis shows $-\log_{10}$ of the BH-adjusted P value from a quasi-Poisson model adjusted for calendar time, day of week, holidays, and same-day Cook County EPA monitor–based daily $PM_{2.5}$. The red dashed line marks BH-adjusted $P = 0.10$. Labels identify the 44 codes meeting all stage 1 criteria. Text labels are displayed for all codes that met all screening criteria: (i) a positive association between ED/UC visit counts and the 3-day moving average of daily maximum temperature, (ii) BH-adjusted $P < 0.1$, (iii) ≥30% of ED/UC visits occurring on days above the 70th percentile of the temperature distribution (29.74°C), and (iv) at least 100 counts of the diagnosis code recorded during warm-season (May to September) in the ED/UC systems. Chapter 19 and 20 (injury/poisoning and external cause) labels are shown in inset boxes to avoid overplotting.

(MRT)—the temperature associated with the lowest estimated risk for that diagnosis, constrained to temperatures at or below the warm-season median [27.60°C (81.68°F)]. Figure 3 displays cumulative odds ratios (ORs) at lags 0 to 3 for diagnosis codes meeting the stage 2 primary reporting criteria: a lower 95% confidence interval (CI) of the cumulative lag 0-to-3 OR entirely above 1 and events per variable (EPV) ≥ 10. Thirty-three diagnoses met the stage 2 numerical reporting criteria. These included 10 disease-related conditions and 23 injury, poisoning, or external-cause conditions.

Among disease-related diagnoses (Fig. 3A), the largest cumulative lag 0-to-3 association was observed for glomerular disorders in diseases classified elsewhere (N08; OR = 11.16; 95% CI: 5.87 to

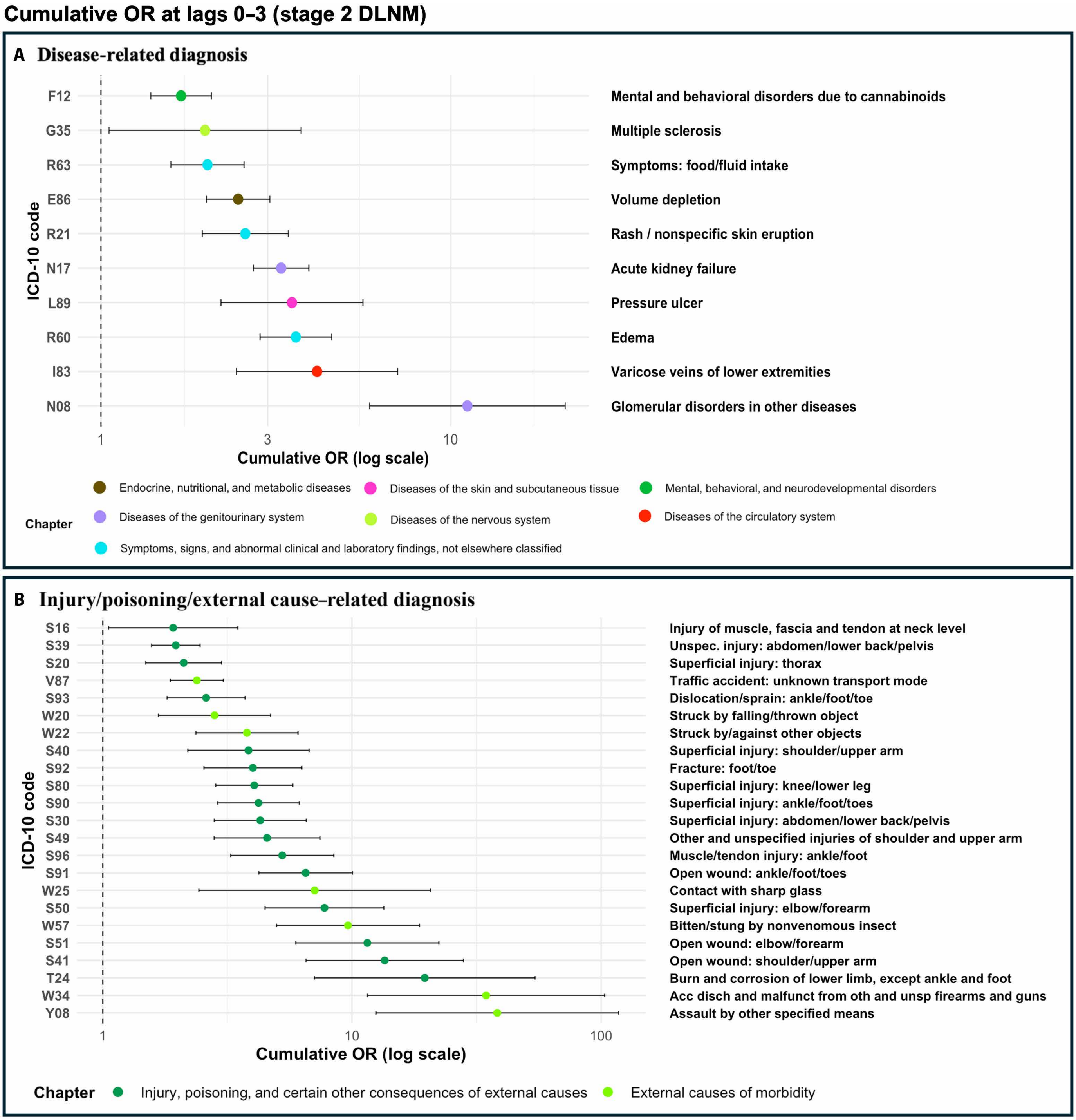

Fig. 3. Cumulative ORs at lags 0 to 3 from stage 2 DLNMs. Points show cumulative ORs at 33.67°C relative to the diagnosis-specific constrained MRT; horizontal bars show 95% CIs. Panel (**A**) presents 10 disease-related diagnoses, and panel (**B**) presents 23 injury, poisoning, and external-cause diagnoses. Reported codes had cumulative lag 0-to-3 lower 95% CI > 1 and EPV ≥ 10. The vertical dashed line marks OR = 1.

21.25). Other associations included varicose veins of the lower extremities (I83; OR = 4.15; 95% CI: 2.44 to 7.05), edema (R60; OR = 3.61; 95% CI: 2.85 to 4.57), pressure ulcer (L89; OR = 3.52; 95% CI: 2.20 to 5.61), acute kidney failure (N17; OR = 3.28; 95% CI: 2.73 to 3.93), rash and other nonspecific skin eruption (R21; OR = 2.59; 95% CI: 1.95 to 3.43), volume depletion (E86; OR = 2.47; 95% CI: 2.00 to 3.04), symptoms concerning food and fluid intake (R63; OR = 2.02; 95% CI: 1.59 to 2.57), multiple sclerosis (G35; OR = 1.99; 95% CI: 1.05 to 3.74), and mental and behavioral disorders due to cannabinoids (F12; OR = 1.69; 95% CI: 1.39 to 2.07). Table 2 summarizes same-day (lag 0) and cumulative (lags 0 to 1, 0 to 2, and 0 to 3) ORs for the 10 disease-related diagnoses, comparing extreme heat [33.67°C (92.60°F)] with each diagnosis code's MRT. Figure 4 presents the DLNM cumulative exposure-response curves for these 10 disease-related diagnoses, illustrating nonlinear, monotonically increasing risk patterns that steepen markedly at extreme high temperatures.

Among injury, poisoning, and external-cause diagnoses (Fig. 3B), the largest cumulative estimates were observed for assault by other specified means (Y08; OR = 38.31; 95% CI: 12.49 to 117.55), accidental firearm discharge (W34; OR = 34.57; 95% CI: 11.56 to 103.40), burn and corrosion of the lower limb (T24; OR = 19.60; 95% CI: 7.07 to 54.33), open wound of the shoulder and upper arm (S41; OR = 13.54; 95% CI: 6.54 to 28.01), and open wound of the elbow and forearm (S51; OR = 11.53; 95% CI: 5.95 to 22.34). The reporting set also included superficial injuries, fractures, sprains, wounds, object-related injuries, contact with sharp glass, nonvenomous insect bites or stings, and traffic accidents. Estimates for uncommon external-cause codes were imprecise and should be interpreted cautiously. Detailed estimates are provided in table S2 and figs. S7 and S8.

Heat-associated diagnoses across demographic and geographic strata

Age-stratified analyses (table S3) identified 11 diagnoses meeting the subgroup reporting criteria among adults aged 18 to 24 years, 25 among those aged 25 to 44 years, 15 among those aged 45 to 64 years, and 13 among adults aged 65 years or older. Five diagnoses were retained across all four age strata: volume depletion (E86), mental and behavioral disorders due to cannabinoids (F12), acute kidney failure (N17), rash and other nonspecific skin eruption (R21), and superficial injury of the knee/lower leg (S80). The 25- to 44-year stratum included additional disease-related codes such as symptoms related to food and fluid intake (R63), multiple sclerosis (G35), and edema (R60), as well as a broader range of injury and external-cause codes. Among the older strata, edema (R60) and varicose veins of the lower extremities (I83) were retained in both the 45 to 64 and 65 years or older strata, and symptoms related to food and fluid intake (R63) and pressure ulcer (L89) were retained among adults aged 65 years or older. Because event counts and estimate precision differed across age strata, these patterns are descriptive and should not be interpreted as formal evidence of age-related differences in heat susceptibility.

Sex-stratified analyses (table S4) retained 27 diagnoses among female patients and 26 among male patients. Twenty-one diagnoses were retained in both strata, spanning renal and fluid-balance diagnoses: volume depletion (E86), acute kidney failure (N17), glomerular disorders in other diseases (N08), edema (R60), symptoms concerning food/fluid intake (R63), rash and other nonspecific skin eruption (R21), pressure ulcer (L89), and multiple injury/external-cause codes. Diagnoses retained only among female patients included multiple sclerosis (G35), mental and behavioral disorders due to cannabinoids (F12), neck muscle/tendon injury (S16), superficial injury of the thorax (S20), dislocations and sprains of the ankle/foot/toes (S93), and struck by falling/thrown object (W20). Diagnoses retained only among male patients included varicose veins of the lower extremities (I83), open wound of the shoulder/upper arm (S41), contact with sharp glass (W25), accidental firearm discharge (W34), and assault by other specified means (Y08). These exploratory findings were not formal tests of effect heterogeneity; therefore, retention in only one stratum should not be interpreted as evidence of a statistically significant difference between female and male patients.

Race/ethnicity–stratified analyses (table S5) retained one diagnosis among Asian patients, 23 among Black or African American patients,

Table 2. Same-day and cumulative lag 0-to-1, 0-to-2, and 0-to-3 ORs (95% CIs) for disease-related diagnoses meeting the stage 2 reporting criteria. Models used a time-stratified case-crossover DLNM adjusted for same-day Cook County EPA monitor–based daily $PM_{2.5}$. Codes are ordered by increasing cumulative lag 0-to-3 OR.

ICD-10 code and description	Same-day OR (lag 0)	Cumulative OR (lags 0 to 1)	Cumulative OR (lags 0 to 2)	Cumulative OR (lags 0 to 3)
Disease-related diagnoses				
F12: Mental and behavioral disorders due to cannabinoids	1.13 (1.04–1.22)	1.29 (1.14–1.46)	1.49 (1.26–1.76)	1.69 (1.39–2.07)
G35: Multiple sclerosis	1.36 (1.02–1.82)	1.61 (1.06–2.45)	1.79 (1.05–3.06)	1.99 (1.05–3.74)
R63: Symptoms and signs concerning food and fluid intake	1.22 (1.09–1.37)	1.46 (1.24–1.71)	1.72 (1.40–2.11)	2.02 (1.59–2.57)
E86: Volume depletion	1.29 (1.17–1.42)	1.63 (1.42–1.88)	2.03 (1.70–2.43)	2.47 (2.00–3.04)
R21: Rash and other nonspecific skin eruption	1.36 (1.19–1.54)	1.72 (1.42–2.08)	2.11 (1.66–2.69)	2.59 (1.95–3.43)
N17: Acute kidney failure	1.43 (1.32–1.56)	1.96 (1.73–2.21)	2.57 (2.20–3.01)	3.28 (2.73–3.93)
L89: Pressure ulcer	1.48 (1.20–1.83)	2.04 (1.49–2.79)	2.70 (1.82–4.03)	3.52 (2.20–5.61)
R60: Edema	1.53 (1.38–1.70)	2.13 (1.82–2.49)	2.80 (2.29–3.43)	3.61 (2.85–4.57)
I83: Varicose veins of lower extremities	1.48 (1.16–1.89)	2.11 (1.49–2.99)	2.96 (1.89–4.64)	4.15 (2.44–7.05)
N08: Glomerular disorders in diseases classified elsewhere	1.76 (1.34–2.31)	3.37 (2.25–5.03)	6.37 (3.73–10.86)	11.16 (5.87–21.25)

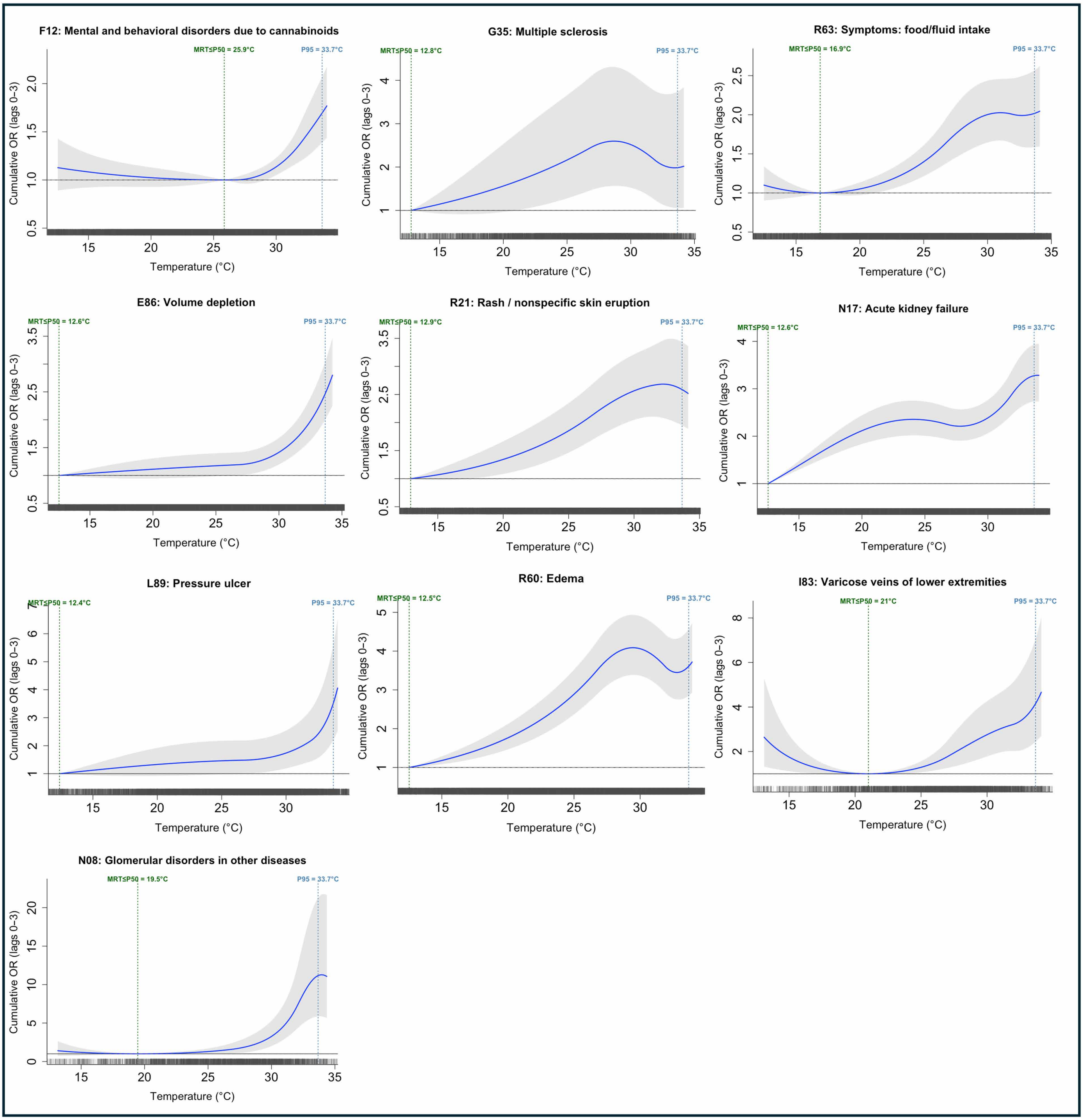

Fig. 4. Cumulative lag 0-to-3 exposure-response associations between temperature and ED/UC (ED) visits for disease-related diagnoses. Cumulative lag 0-to-3 temperature-ED associations estimated with DLNMs in a time-stratified case-crossover design for the 10 disease-related diagnosis codes meeting the primary selection criterion. Curves show cumulative ORs across the observed warm-season temperature range, with shaded bands representing 95% CIs. Each panel reports the MRT and the 95th percentile of daily maximum temperature [33.67°C (92.60°F); P95]. The horizontal dashed line marks OR = 1. Diagnoses are ordered from smallest to largest cumulative OR at extreme heat.

12 among patients in the other race/ethnicity group, and 22 among white patients. Volume depletion (E86) was retained in all four strata. Acute kidney failure (N17), rash and other nonspecific skin eruption (R21), edema (R60), symptoms concerning food/fluid intake (R63), unspecified injury of the abdomen/lower back/pelvis (S39), superficial injury of the knee/lower leg (S80), superficial injury of the ankle/foot/toes (S90), dislocations and sprains of the ankle/foot/toes (S93), and traffic accident with unknown transport mode (V87) were retained among Black or African American, other, and white patients. Beyond these shared diagnoses, the Black or African American and white strata included a broader range of injury-related and external-cause codes, including open wounds, superficial injuries, muscle/tendon injuries, fractures, object- or glass-related injuries, and insect bites or stings. Some retained diagnoses were more restricted to specific strata, including glomerular disorders in other diseases (N08) among Black or African American patients and varicose veins of the lower extremities (I83) and pressure ulcer (L89) among white patients. The smaller number of retained diagnoses among Asian patients should be interpreted in light of smaller event counts and limited statistical precision and should not be interpreted as evidence of lower heat susceptibility.

Diagnoses were distributed across geographic regions, with no code retained in all seven regions (table S6). Acute kidney failure (N17) and edema (R60) were retained in six regions, while volume depletion (E86), mental and behavioral disorders due to cannabinoids (F12), and dislocations and sprains of the ankle/foot/toes (S93) were retained in five regions. The West Side had the broadest retained set, including glomerular disorders in other diseases (N08), varicose veins of the lower extremities (I83), multiple sclerosis (G35), and several injury-related or external-cause codes. These patterns are descriptive and should not be interpreted as formal evidence of geographic differences in heat susceptibility.

Sensitivity analysis

We conducted five groups of sensitivity analyses to examine the influence of model specification, stage 1 screening thresholds, warm-season definition, recurrent health care use, and the $PM_{2.5}$ data source (Table 3). Under alternative stage 2 temperature-knot specifications, all 33 primary diagnoses were retained with a single 50th-percentile knot, 30 were retained with 70th- and 90th-percentile knots, and 29 were retained with 50th-, 70th-, and 90th-percentile knots. G35, S16, and Y08 were not retained under the 70th/90th-percentile specification; G35, S16, T24, and Y08 were not retained under the three-knot specification. Thus, most of the stage 2 reporting set was preserved across knot specifications, although several diagnoses were sensitive to this modeling choice.

Changing the stage 1 minimum count from 100 to 50 did not alter the 33-diagnosis stage 2 reporting set. Relaxing the stage 1 relative-frequency threshold from ≥30 to ≥20% retained all primary diagnoses and added 24, producing a 57-diagnosis stage 2 reporting set. Applying a stricter stage 1 BH-FDR threshold of $q \leq 0.05$ retained 18 of the 33 primary diagnoses at stage 2. These results indicate that the final reporting set was unchanged by the lower count threshold but was more sensitive to the relative-frequency and FDR thresholds used during stage 1 screening.

Restricting both stages to June to August and recomputing stage 1 screening within this restricted window yielded seven stage 1 candidates and one clinical stage 2 reporting diagnosis: volume depletion (E86; OR = 2.60; 95% CI: 2.16 to 3.12). In this restricted analysis, the stage 1 relative-frequency criterion was recalculated using the June-to-August 70th-percentile temperature of 30.64°C, and the stage 2 extreme-heat contrast was evaluated at the June-to-August 95th-percentile temperature of 34.13°C. No diagnosis was newly detected relative to the primary analysis. The reduced reporting set reflects the narrower exposure window, June to August–specific stage 1 count and relative-frequency screening, recalculated temperature thresholds, and stage 2 precision/stability criteria, rather than $PM_{2.5}$ adjustment alone. After excluding patients with at least five summer ED/UC visits, 24 of the 33 primary diagnoses remained; G35, L89, N08, S16, T24, W20, W25, W34, and Y08 were not retained. The retention of most primary diagnoses after this exclusion suggests that the overall reporting set was not driven solely by patients with frequent acute-care use.

To evaluate whether diagnosis selection and stage 2 effect estimates were sensitive to the $PM_{2.5}$ exposure data source, we conducted a sensitivity analysis restricted to 2011 to 2021, the period during which the long-term gap-free high-resolution air pollutants (LGHAP) global daily $PM_{2.5}$ (*54*) product provided spatially resolved gridded estimates that could be linked to patient residential census tracts and compared with EPA monitor–based daily $PM_{2.5}$ (*44*). The main finding was that estimates for overlapping diagnoses were similar across $PM_{2.5}$ data sources, while the shorter 2011-to-2021 study period accounted for much of the reduction in the retained diagnosis set relative to the primary 2011-to-2023 analysis. The LGHAP-adjusted analysis retained 20 stage 2 reporting diagnoses, and the same-period EPA-adjusted analysis retained 22; 19 diagnoses overlapped between the two analyses. Compared with the primary 2011-to-2023 EPA-adjusted analysis, the LGHAP sensitivity analysis did not retain 17 of the 33 primary diagnoses and identified four sensitivity-only diagnoses (I77, M48, S71, and W50). Source-specific differences were limited: W50 was retained only in the LGHAP-adjusted analysis, whereas S51, S96, and W34 were retained only in the same-period EPA-adjusted analysis. These findings suggest that the reduced LGHAP sensitivity set was driven primarily by restriction to 2011 to 2021 rather than by the use of the gridded $PM_{2.5}$ product itself.

DISCUSSION

We conducted an exploratory HWAS to characterize adult ED/UC diagnoses associated with extreme heat across four Chicago health care systems. Among 916,904 visits from 372,140 adults during May to September 2011 to 2023, daily EPA $PM_{2.5}$-adjusted stage 1 screening retained 44 codes. Thirty-three diagnoses met the stage 2 numerical criteria: 10 disease-related conditions and 23 injury, poisoning, or external-cause conditions.

Our study provides a broad, complementary characterization of heat-associated morbidity that reinforces the existing literature. Excessive heat exposure has been shown to be associated with a broad range of diagnostic categories, including renal, cardiovascular, respiratory, electrolyte, and mental disorders (*20*–*24*, *26*–*28*, *47*), as well as injury-related diagnoses (*7*, *29*). However, to our knowledge, no prior studies have systematically assessed individual-level diagnosis codes from ED records across the broader adult population. By screening across all 1803 ICD-10 categories rather than relying on a prespecified outcome set, our HWAS framework captures the full breadth of heat-sensitive clinical presentations in acute-care settings.

Among disease-related diagnoses, renal and fluid-balance signals—volume depletion, acute kidney failure, edema, and glomerular

Table 3. Summary of sensitivity analyses. Primary stage 2 reporting included 33 diagnoses. RF, relative frequency; BSA, body surface area; NOS, not otherwise specified.

Sensitivity analysis	Dropped from primary	Newly detected (sensitivity-only)
(1a) DLNM knot at 50th percentile only (vs primary: 50th + 90th)	–	–
(1b) DLNM knots at 70th and 90th percentiles (vs primary: 50th + 90th)	Disease (1): G35	–
	Injury/ext (2): S16, Y08	
(1c) DLNM knots at 50th, 70th, and 90th percentiles (vs primary: 50th + 90th)	Disease (1): G35	–
	Injury/ext (3): S16, T24, Y08	
(2a) Stage 1 count ≥50 (vs primary: ≥100)	–	–
(2b) Stage 1 relative frequency ≥20% (vs primary: ≥30%)	–	Disease (12): B18 (*chronic viral hepatitis*), D50 (*iron deficiency anemia*), E11 (*type 2 diabetes*), I65 (*precerebral artery stenosis/occlusion*), J30 (*allergic rhinitis*), J45 (*asthma*), L50 (*urticaria*), M19 (*osteoarthritis*), M25 (*joint disorders*), M79 (*soft tissue disorders*), N18 (*chronic kidney disease*), N28 (*other kidney/ureter disorders*)
		Injury/ext (12): S01, S59, S61, S69, S70, S89, S99, T07, W18, W26, Y92, Y93
(2c) Stage 1 BH-FDR $q \leq 0.05$ (vs primary: $q < 0.10$)	Disease (5): F12, G35, I83, L89, N08	–
	Injury/ext (10): S16, S20, S49, S93, S96, T24, W20, W22, W34, Y08	
(3) Both stages restricted to June–August	Disease (9): F12, G35, I83, L89, N08, N17, R21, R60, R63	–
	Injury/ext (23): S16, S20, S30, S39, S40, S41, S49, S50, S51, S80, S90, S91, S92, S93, S96, T24, V87, W20, W22, W25, W34, W57, Y08	
(4) Excluding patients with ≥5 summer ED/UC visits	Disease (3): G35, L89, N08	–
	Injury/ext (6): S16, T24, W20, W25, W34, Y08	
(5) LGHAP gridded daily $PM_{2.5}$, 2011–2021	Disease (6): G35, I83, N08, N17, R21, R63	Disease (2): I77 (*other arterial disorders*), M48 (*other spinal disorders*)
	Injury/ext (11): S16, S20, S30, S39, S49, S51, S93, S96, W22, W34, Y08	Injury/ext (2): S71 (*hip/thigh open wound*), W50 (*assault/struck by person*)

disorders—were prominent, consistent with prior evidence of dehydration and renal stress during heat exposure. Pressure ulcer, nonspecific skin eruption, multiple sclerosis, and cannabinoid-related disorders were also retained. Varicose veins of the lower extremities was the only circulatory diagnosis retained; no acute cardiovascular diagnosis met the reporting criteria. No respiratory diagnosis met the reporting criteria. Differences in care setting, outcome definition, and population may contribute to this pattern, and the result should not be interpreted as evidence that heat lacks cardiovascular effects.

Our study also contributes to the growing recognition of heat-associated trauma and behavioral diagnoses. The identification of a broad range of injury, poisoning, and external-cause codes—including open wounds, superficial injuries, assaults, and accidental firearm discharge—reinforces existing evidence that extreme heat increases the risk of accidental and violent injuries (*7*, *29*, *49*). Several assault-related codes showed elevated point estimates in the expected direction, although some were accompanied by wide CIs, indicating limited precision in the magnitude of these associations. These findings should therefore be interpreted cautiously as suggestive patterns that are broadly consistent with prior literature linking elevated temperatures to aggression and violence-related outcomes (*49*–*52*). Beyond the cannabis-related behavioral disorders captured in our analysis, most common psychiatric diagnoses were not retained in the primary reporting set. Prior studies have independently linked elevated temperatures to injury- and assault-related presentations and to psychiatric or mental health–related encounters (*50*, *51*, *53*, *48*), but in this ED-based analysis, injury- and assault-related codes were more prominent than primary psychiatric diagnoses.

Together, these findings reinforce established heat-health associations and extend their clinical description across an all-comer adult acute-care dataset. The HWAS framework offers a complementary method for prioritizing diagnoses without prespecifying an outcome list. Associations for less commonly studied diagnoses should be treated as signals for targeted replication rather than definitive new causal relationships.

Sensitivity analyses suggested that the primary findings were generally stable across alternative stage 2 model specifications but more sensitive to screening stringency and seasonal restriction. Most of the 33 primary stage 2 reporting diagnoses were retained when the DLNM temperature-response spline was reparameterized: All 33 were retained with a single 50th-percentile knot, 30 were retained with knots at the 70th and 90th percentiles, and 29 were retained with knots at the 50th, 70th, and 90th percentiles. Similarly, lowering the stage 1 minimum count threshold from 100 to 50 did not change the

33-diagnosis reporting set. In contrast, relaxing the stage 1 relative-frequency criterion to ≥20% expanded the reporting set to 57 diagnoses, whereas applying a stricter stage 1 BH-FDR threshold of $q < 0.05$ retained 18 diagnoses. Restricting both stages to June to August retained only volume depletion (E86), consistent with the narrower exposure window, recalculated temperature thresholds, and reduced event counts. This result indicates that several May-to-September findings, particularly injury and external-cause diagnoses, were sensitive to the exposure-domain definition and should be interpreted as exploratory warm-season signals rather than robust heat-associated outcomes. After excluding frequent acute-care users, 24 of the 33 primary diagnoses remained, suggesting that the overall reporting set was not driven solely by patients with repeated ED/UC visits, although several less precise disease and injury/external-cause signals were attenuated. Last, when the study period was held constant at 2011 to 2021, EPA monitor–based and LGHAP gridded daily $PM_{2.5}$ analyses produced broadly similar but not identical stage 2 reporting sets (22 and 20 diagnoses, respectively; 19 overlapping diagnoses), with similar estimates for overlapping diagnoses. This pattern suggests that the reduced LGHAP sensitivity set primarily reflects restriction to the shorter 2011-to-2021 period rather than a strong dependence on the $PM_{2.5}$ data source alone.

Despite our study's strengths, several limitations should be acknowledged. First, our analysis was confined to adults using four health care systems within the dense urban environment of Chicago. Our EHR cohort was skewed in demographic composition—Black, female, and West Side patients were overrepresented, while white and Northwest Side patients were underrepresented. This apparent underrepresentation likely reflects the geographic concentration of our cohort and differences in racial classification between EHR and Census instruments. These imbalances in EHR cohort composition may have constrained the precision of subgroup analyses and limit the generalizability of our findings to populations not well represented in the dataset but indicate differences in health care utilization, coverage, and health burden across Chicago.

A second limitation concerns heat exposure assessment and the absence of socioeconomic variables. We linked patient residential census tracts to ambient temperature under the assumption that this best represents individual exposure. However, this approach does not account for intracity movement, occupational environments, time spent indoors, or access to air conditioning during heat events. The omission of socioeconomic indicators such as income, education, and housing quality raises the potential for residual confounding and may obscure the impact of structural inequities on heat-related health risks.

The third limitation is that gridded daily $PM_{2.5}$ data were not available for the full study period, including 2022–2023. Therefore, in the primary analyses, $PM_{2.5}$ adjustment used a Cook County daily mean derived from EPA (*44*), which captured day-to-day temporal variation but assigned the same value across census tracts and did not capture within-county spatial contrasts. To evaluate the potential influence of this choice, we conducted a sensitivity analysis restricted to 2011 to 2021, the period for which both EPA-based daily county mean $PM_{2.5}$ and LGHAP gridded daily $PM_{2.5}$ data (*54*) were available, and compared results using the two $PM_{2.5}$ adjustment approaches.

In addition, this study did not include external validation or independent replication because stage 1 screening and stage 2 characterization were applied to the same underlying cohort. Therefore, the stage 2 estimates should not be interpreted as confirmatory post–selection inference. Replication of the full framework in independent acute-care datasets from other geographic settings is further needed to assess the robustness of the retained associations and to characterize the method's utility across populations, climates, coding practices, and health care systems.

Last, the structure of our health care utilization data presents certain constraints. We relied on cross-sectional ED visit data rather than longitudinal patient records, precluding our ability to track cumulative heat impacts, recurrent hospitalizations, or the modifying influence of long-term health conditions and medication use. The dataset included more than 900,000 visits from ∼372,000 unique patients, indicating a substantial proportion of frequent users of acute-care services. While our case-crossover design inherently controls for fixed individual-level confounders and mitigates the influence of repeat utilization through within-person matching, our estimates may still disproportionately reflect outcomes among high-user subpopulations. In addition, as documented in figs. S1 to S6, the analytic cohort was not compositionally static across the study period; annual visit volume, site composition, patient demographic composition, and the distribution of diagnosis chapters each varied across calendar years. Although the stage 1 quasi-Poisson models included a flexible calendar-time spline and the stage 2 case-crossover design controls for within-stratum temporal confounding, residual confounding from unmeasured shifts in case mix—such as changes in site-level coding thresholds, institutional practice patterns, or patient population composition—cannot be fully excluded. From a clinical informatics perspective, our reliance on individual ICD-10 diagnosis codes introduces challenges related to coding practices, as coding practices varied across contributing health care systems and may reflect clinician behaviors and include rule-out diagnoses. ICD-10 coding heterogeneity across institutions and providers introduces an additional challenge: The same clinical presentation may be coded differently depending on institutional billing conventions, provider specialty, or documentation practices.

In summary, this large-scale citywide HWAS suggests that extreme heat is associated with increased ED presentations extending well beyond classical heat illness, encompassing acute kidney failure, fluid and electrolyte disturbances, dermatologic-related conditions, multiple sclerosis, cannabinoid-related disorders, varicose veins of the lower extremities, and a broad range of injury, poisoning, and external-cause diagnoses. These findings may have public health relevance: Heat emergency response plans could consider clinical alerts not only for heat illness but also for renal and fluid-balance complications that may manifest with a physiological lag of several days; EDs and UC clinics may anticipate an increased demand for dehydration- and renal-related care during and after extreme heat events, and injury prevention messaging—including outdoor safety guidance issued during heat alerts—may help reduce the burden of heat-associated trauma. By presenting a data-driven characterization of heat-sensitive clinical conditions, this study supports targeted clinical preparedness and future validation of heat-related health outcomes.

MATERIALS AND METHODS

Data

We used ED encounters captured in CAPriCORN (*42*) EHR data from four health care systems to construct a Chicago citywide cohort of ED encounters among adult patients (916,904 ED visits;

372,140 unique patients). Inclusion criteria included ED visits by adults (aged ≥18 years) who sought care at a CAPriCORN-affiliated institution, with geocoded residence located within Cook County, Illinois (the county that includes the City of Chicago), during the warm season, May through September (*55*, *56*), of 2011 to 2023 and with valid ICD-10 diagnostic codes. Because our study period included the transition from ICD-9 to ICD-10 codes (mandated in the US by 1 October 2015), to standardize the diagnoses, we mapped the ICD-9 codes to their corresponding ICD-10 codes using the Centers for Medicare and Medicaid Services General Equivalence Mappings guidance and removed the duplicate codes within each ED encounter. This process yielded a final set of ICD-10 diagnosis codes (n = 1803 distinct categories) extracted from the EHRs. We chose ICD-10 (*57*) as the analytic standard because it provides more granular and internationally recognized diagnostic classifications, which improves consistency across sites and time periods. Although ICD codes are primarily designed for billing in the US, they are widely leveraged in epidemiological and health service research.

Patient characteristics were stratified by sex (female, male, and other), age group (18 to 24, 25 to 44, 45 to 64, and ≥65 years), and race/ethnicity (Asian, Black or African American, white, and other). These categorizations followed the standardized demographic classifications used within CAPriCORN (*42*). For race/ethnicity, groups with relatively small representation—American Indian or Alaska Native (0.6%), Native Hawaiian or other Pacific Islander (0.2%), and individuals reporting multiple races (0.3%)—were aggregated into the "other" category. For the geographic region of residence, we stratified the region into seven Chicago Department of Public Health planning regions—Central, North, Northwest, South, Southwest, Far South, and West Side—on the basis of census tract centroid geography (*58*). A visualization of the region stratification is provided in the Supplementary Materials (fig. S9).

For exposure assessment, daily temperature data were sourced from Daymet (*59*) and linked to the census tract of each patient's residential address at the encounter date. Daily maximum air temperature estimates from Daymet 1-km grid cells within each tract were averaged. Extreme heat was defined as the warm-season 95th percentile (33.67°C), consistent with prior studies (*19*, *60*, *61*). For $PM_{2.5}$ adjustment, we obtained daily measurements from Cook County US EPA Air Quality System monitors (*44*). We averaged same-day Cook County monitors to obtain a daily county mean; the same daily value was assigned to all tracts. This time-varying $PM_{2.5}$ covariate was used in both analytical stages.

Cohort representativeness assessment

To quantify the degree to which the EHR analytic cohort represents the Chicago adult population, we compared the pooled 2011-to-2023 EHR cohort composition to period-matched Census reference estimates for each domain. For age and sex, we used annual American Community Survey (ACS) 1-year estimates from the Selected Population Profile (S0101) for Chicago city, extracted for each available year from 2011 to 2023 (excluding 2020, for which 1-year estimates were not released). Reference proportions for four age groups (18 to 24, 25 to 44, 45 to 64, and ≥65 years) and sex (female and male) among adults 18 years and older were averaged across all available years to produce a period-matched reference spanning the full study period. This approach accounts for Chicago's shifting demographic structure over the 13-year study window, most notably the increase in the 65+-year adult share from 13.1% in 2011 to 17.7% in 2023.

For race/ethnicity, we used annual B02001 Race estimates from the ACS for Chicago city, averaged across 2011 to 2019 (9 years, pre-redesign). The 2021 ACS race question redesign introduced a structural discontinuity, making post-2021 data incompatible with pre-2021 estimates (*62*). Accordingly, we used the 2011-to-2019 pre-redesign average as the race reference, which aligns with the EHR coding period and avoids mixing incompatible measurement frameworks. Race categories (white, Black or African American, Asian, and other) were matched to EHR race codes.

For the geographic region, we used ACS 5-year Demographic and Housing Characteristics (DP05) at the census tract level for Cook County (Illinois), for three successive 5-year periods: 2011 to 2015, 2014 to 2018, and 2019 to 2023. Tracts were geocoded to one of Chicago's 77 community areas, and each community area was linked to one of the seven study regions (Central, North Side, Northwest Side, West Side, South Side, Southwest Side, and Far South Side). Adult population counts within each region were summed across constituent tracts, and the region's share of the total Chicago population was computed for each 5-year period; the three-period average was used as the reference distribution.

EHR proportions were computed among all unique patients with nonmissing values; the difference (EHR cohort composition minus Census reference average, in percentage points) was used as the representativeness metric, computed separately for each domain. The temporal stability of the Census reference population was assessed by examining year-over-year and period-over-period changes in each demographic characteristic to confirm that a single averaged reference was appropriate for the full 2011-to-2023 study period.

Statistical analysis

To comprehensively assess acute-care diagnoses associated with extreme heat, we applied an HWAS design across 1803 ICD-10 diagnosis categories. This approach systematically screened diagnosis codes for an extreme heat association rather than restricting analyses to a limited set of prespecified outcomes, allowing broad characterization of heat-sensitive clinical presentations. Given the large number of ED/UC diagnosis codes, we used a two-stage analytic strategy. In stage 1, we conducted a screening procedure using diagnosis-specific quasi-Poisson regression to identify temperature-sensitive diagnoses while accounting for overdispersed daily ED/UC visit counts. For each ICD-10 code, the daily count of ED/UC visits with that code served as the outcome. The exposure was the 3-day moving average of citywide daily maximum temperature (average of same-day, lag 1, and lag 2 temperatures), which captures cumulative thermal burden over the preceding days and reduces day-to-day variability relative to a single-day measure. Models included a natural cubic spline of calendar time with 4 degrees of freedom per year (*63*, *64*), indicators for day of week and federal holidays, and same-day Cook County mean $PM_{2.5}$ derived from EPA monitors (*44*).

Codes were retained if they met the following criteria: (i) They had a positive temperature coefficient (*45*), (ii) BH-adjusted $P < 0.10$, (iii) at least 30% of ED/UC visits for that diagnosis occurred on days when the daily maximum temperature exceeded the warm-season 70th percentile threshold (29.74°C), and (iv) at least 100 counts of the diagnosis code were recorded during the warm season in the ED/UC systems. We used the 70th percentile (29.74°C) of the warm-season temperature distribution to capture commonly experienced, rather than rare, temperature extremes for the first screening stage. In parallel, the requirement that at least 30% of visits for a given code occurred on days above the 70th percentile temperature threshold served as a support criterion to ensure sufficient observations under warm conditions and to limit signals driven by a few extreme heat days.

In stage 2, the resulting candidate diagnoses identified from stage 1 were analyzed individually using DLNMs within a time-stratified case-crossover design (*13*), with strata defined by calendar month and year and control days matched to case days within the same stratum. In the case-crossover framework, each ED/UC visit served as its own case day, with control days sampled from the same day of week in the same calendar month to account for seasonal and long-term temporal trends. This design inherently controls for time-invariant individual- and area-level confounders. The model additionally adjusted for same-day Cook County EPA monitor–based daily $PM_{2.5}$ (*44*). The daily maximum temperature was modeled with a DLNM cross-basis to capture both nonlinear exposure-response and distributed lag effects. The exposure dimension used a quadratic B-spline with two internal knots placed at the diagnosis-specific 50th and 90th percentiles of the observed temperature distribution across all case and control days, with boundary knots set at the 2.5th and 97.5th percentiles of the same distribution (*65*, *66*). The lag dimension used a natural spline over lags 0 to 3 days with a single internal knot placed on the log-transformed lag scale, concentrating flexibility at shorter time lags, typical of heat-related acute-care presentations (*19*, *67*, *68*). The MRT, defined as the temperature associated with the lowest cumulative OR across the exposure-response curve, was identified from the cumulative exposure-response function and constrained to temperatures at or below the warm-season median. We present codes from the second stage that met a primary selection criterion: cumulative lag 0-to-3 lower 95% CI > 1 and EPV ≥ 10.

To evaluate potential effect modification by demographic and geographic factors, we performed exploratory stratified analyses retaining the primary stage 2 DLNM specification and EPA daily $PM_{2.5}$ adjustment. Cumulative and lag-specific ORs were estimated separately within strata defined by patient sex (female, male, and other), age group (18 to 24, 25 to 44, 45 to 64, and ≥65 years), race/ethnicity (Asian, Black or African American, white, and other), and geographic region of residence (Central, North, Northwest, South, Southwest, Far South, and West Side Chicago). Within each stratum, we refit the stage 2 model for all 44 stage 1 candidates and applied the primary temperature basis, lag structure, constrained-MRT rule, and stage 2 numerical reporting criteria. The subgroup results were used for a descriptive comparison rather than formal interaction testing.

We conducted five groups of sensitivity analyses. First, to assess sensitivity to internal knot placement in the DLNM exposure-response spline, stage 2 models were reestimated under three alternative specifications: a single internal knot at the 50th percentile, two knots at the 70th and 90th percentiles, and three knots at the 50th, 70th, and 90th percentiles of the diagnosis-specific observed temperature distribution across all case and control days. Second, to evaluate sensitivity to stage 1 inclusion thresholds, we repeated the two-stage analysis under four alternative criteria: lowering the minimum case count from at least 100 to at least 50 visits, raising the relative-frequency criterion from at least 30% to more than 40% of visits on days exceeding the 70th temperature percentile, relaxing the relative-frequency criterion to more than 20%, and applying a stricter FDR threshold of $q < 0.05$. For all stage 1 sensitivity analyses, stage 2 was rerun with the primary specification. Third, both stages were restricted to the peak summer months (June to August), with the temperature and frequency thresholds recomputed for this narrower warm-season window. Fourth, to evaluate whether heat-susceptible diagnoses were driven by patients with repeated ED/UC visits, stage 2 was refit after excluding patients with at least five summer ED/UC visits. These analyses used EPA monitor–based daily $PM_{2.5}$ in both applicable stages. Last, because LGHAP gridded daily $PM_{2.5}$ was available only through 2021, we repeated the full two-stage analysis during 2011 to 2021 using both LGHAP gridded daily $PM_{2.5}$ (*54*) and EPA monitor–based daily $PM_{2.5}$ (*44*) to assess whether the retained diagnosis set and stage 2 effect estimates were sensitive to the choice of $PM_{2.5}$ exposure data source over an identical study period.

Supplementary Materials

This PDF file includes:
Figs. S1 to S9
Tables S1 to S6

REFERENCES

1. A. R. Crimmins, C. W. Avery, D. R. Easterling, K. E. Kunkel, B. C. Stewart, T. K. Maycock, *The Fifth National Climate Assessment* (US Global Change Research Program, 2023).
2. K. L. Ebi, A. Capon, P. Berry, C. Broderick, R. de Dear, G. Havenith, Y. Honda, R. S. Kovats, W. Ma, A. Malik, N. B. Morris, L. Nybo, S. I. Seneviratne, J. Vanos, O. Jay, Hot weather and heat extremes: Health risks. *Lancet* **398**, 698–708 (2021).
3. C. Mora, B. Dousset, I. R. Caldwell, F. E. Powell, R. C. Geronimo, C. R. Bielecki, C. W. Counsell, B. S. Dietrich, E. T. Johnston, L. V. Louis, M. P. Lucas, M. M. McKenzie, A. G. Shea, H. Tseng, T. W. Giambelluca, L. R. Leon, E. Hawkins, C. Trauernicht, Global risk of deadly heat. *Nat. Clim. Change* **7**, 501–506 (2017).
4. S. Legg, IPCC, 2021: Climate change 2021-the physical science basis. *Interaction* **49**, 44–45 (2021).
5. A. Hsu, G. Sheriff, T. Chakraborty, D. Manya, Disproportionate exposure to urban heat island intensity across major US cities. *Nat. Commun.* **12**, 2721 (2021).
6. A. Mohajerani, J. Bakaric, T. Jeffrey-Bailey, The urban heat island effect, its causes, and mitigation, with reference to the thermal properties of asphalt concrete. *J. Environ. Manage.* **197**, 522–538 (2017).
7. R. M. Parks, J. E. Bennett, H. Tamura-Wicks, V. Kontis, R. Toumi, G. Danaei, M. Ezzati, Anomalously warm temperatures are associated with increased injury deaths. *Nat. Med.* **26**, 65–70 (2020).
8. R. E. Davis, P. C. Knappenberger, P. J. Michaels, W. M. Novicoff, Changing heat-related mortality in the United States. *Environ. Health Perspect.* **111**, 1712–1718 (2003).
9. R. Kaiser, A. Le Tertre, J. Schwartz, C. A. Gotway, W. R. Daley, C. H. Rubin, The effect of the 1995 heat wave in Chicago on all-cause and cause-specific mortality. *Am. J. Public Health* **97**, S158–S162 (2007).
10. D. O. Astrom, B. Forsberg, J. Rocklov, Heat wave impact on morbidity and mortality in the elderly population: A review of recent studies. *Maturitas* **69**, 99–105 (2011).
11. X. Basagana, C. Sartini, J. Barrera-Gomez, P. Dadvand, J. Cunillera, B. Ostro, J. Sunyer, M. Medina-Ramon, Heat waves and cause-specific mortality at all ages. *Epidemiology* **22**, 765–772 (2011).
12. J. Cheng, Z. Xu, H. Bambrick, H. Su, S. Tong, W. Hu, Heatwave and elderly mortality: An evaluation of death burden and health costs considering short-term mortality displacement. *Environ. Int.* **115**, 334–342 (2018).
13. Y. Guo, A. G. Barnett, X. Pan, W. Yu, S. Tong, The impact of temperature on mortality in Tianjin, China: A case-crossover design with a distributed lag nonlinear model. *Environ. Health Perspect.* **119**, 1719–1725 (2011).
14. N. Scovronick, F. Sera, B. Vu, A. M. Vicedo-Cabrera, D. Roye, A. Tobias, X. Seposo, B. Forsberg, Y. Guo, S. Li, Y. Honda, R. Abrutzky, M. de Sousa Zanotti, S. Coelho, P. H. N. Saldiva, E. Lavigne, H. Kan, S. Osorio, J. Kysely, A. Urban, H. Orru, E. Indermitte, J. J. Jaakkola, N. Ryti, M. Pascal, K. Katsouyanni, F. Mayvaneh, A. Entezari, P. Goodman, A. Zeka, P. Michelozzi, F. de'Donato, M. Hashizume, B. Alahmad, A. Zanobetti, J. Schwartz, M. H. Diaz, C. De La Cruz Valencia, S. Rao, J. Madureira, F. Acquaotta, H. Kim, W. Lee, C. Iniguez, M. S. Ragettli, Y. L. Guo, T. N. Dang, D. V. Dung, B. Armstrong, A. Gasparrini, Temperature-mortality associations by age and cause: A multi-country multi-city study. *Environ. Epidemiol.* **8**, e336 (2024).
15. D. M. Hondula, R. E. Davis, M. V. Saha, C. R. Wegner, L. M. Veazey, Geographic dimensions of heat-related mortality in seven U.S. cities. *Environ. Res.* **138**, 439–452 (2015).
16. K. Knowlton, M. Rotkin-Ellman, G. King, H. G. Margolis, D. Smith, G. Solomon, R. Trent, P. English, The 2006 California heat wave: Impacts on hospitalizations and emergency department visits. *Environ. Health Perspect.* **117**, 61–67 (2009).

17. P. J. Schramm, A. Vaidyanathan, L. Radhakrishnan, A. Gates, K. Hartnett, P. Breysse, Heat-related emergency department visits during the Northwestern heat wave—United States, June 2021. *MMWR Morb. Mortal. Wkly Rep.* **70**, 1020–1021 (2021).
18. J. J. Hess, S. Saha, G. Luber, Summertime acute heat illness in U.S. emergency departments from 2006 through 2010: Analysis of a nationally representative sample. *Environ. Health Perspect.* **122**, 1209–1215 (2014).
19. S. Sun, K. R. Weinberger, A. Nori-Sarma, K. R. Spangler, Y. Sun, F. Dominici, G. A. Wellenius, Ambient heat and risks of emergency department visits among adults in the United States: Time stratified case crossover study. *BMJ* **375**, e065653 (2021).
20. A. L. Braga, A. Zanobetti, J. Schwartz, The effect of weather on respiratory and cardiovascular deaths in 12 U.S. cities. *Environ. Health Perspect.* **110**, 859–863 (2002).
21. F. Ye, W. T. Piver, M. Ando, C. J. Portier, Effects of temperature and air pollutants on cardiovascular and respiratory diseases for males and females older than 65 years of age in Tokyo, July and August 1980–1995. *Environ. Health Perspect.* **109**, 355–359 (2001).
22. S. Lin, M. Luo, R. J. Walker, X. Liu, S. A. Hwang, R. Chinery, Extreme high temperatures and hospital admissions for respiratory and cardiovascular diseases. *Epidemiology* **20**, 738–746 (2009).
23. B. Wen, R. Xu, Y. Wu, M. Coelho, P. H. N. Saldiva, Y. Guo, S. Li, Association between ambient temperature and hospitalization for renal diseases in Brazil during 2000–2015: A nationwide case-crossover study. *Lancet Reg. Health Am.* **6**, 100101 (2022).
24. Y. Qu, W. Zhang, A. M. Boutelle, I. Ryan, X. Deng, X. Liu, S. Lin, Associations between ambient extreme heat exposure and emergency department visits related to kidney disease. *Am. J. Kidney Dis.* **81**, 507–516.e1 (2023).
25. A. L. Hansen, P. Bi, P. Ryan, M. Nitschke, D. Pisaniello, G. Tucker, The effect of heat waves on hospital admissions for renal disease in a temperate city of Australia. *Int. J. Epidemiol.* **37**, 1359–1365 (2008).
26. M. Prpic, C. Hoffmann, W. Bauer, P. Hoffmann, K. Kappert, Urban heat and burden of hyponatremia. *JAMA Netw. Open* **7**, e2450280 (2024).
27. R. Thompson, E. L. Lawrance, L. F. Roberts, K. Grailey, H. Ashrafian, H. Maheswaran, M. B. Toledano, A. Darzi, Ambient temperature and mental health: A systematic review and meta-analysis. *Lancet Planet Health* **7**, e580–e589 (2023).
28. J. Liu, B. M. Varghese, A. Hansen, J. Xiang, Y. Zhang, K. Dear, M. Gourley, T. Driscoll, G. Morgan, A. Capon, P. Bi, Is there an association between hot weather and poor mental health outcomes? A systematic review and meta-analysis. *Environ. Int.* **153**, 106533 (2021).
29. H. Lee, W. Myung, H. Kim, E. M. Lee, H. Kim, Association between ambient temperature and injury by intentions and mechanisms: A case-crossover design with a distributed lag nonlinear model. *Sci. Total Environ.* **746**, 141261 (2020).
30. J. F. Bobb, Z. Obermeyer, Y. Wang, F. Dominici, Cause-specific risk of hospital admission related to extreme heat in older adults. *JAMA* **312**, 2659–2667 (2014).
31. A. S. Bernstein, S. Sun, K. R. Weinberger, K. R. Spangler, P. E. Sheffield, G. A. Wellenius, Warm season and emergency department visits to U.S. children's hospitals. *Environ. Health Perspect.* **130**, 17001 (2022).
32. R. S. Green, R. Basu, B. Malig, R. Broadwin, J. J. Kim, B. Ostro, The effect of temperature on hospital admissions in nine California counties. *Int. J. Public Health* **55**, 113–121 (2010).
33. J. C. Semenza, J. E. McCullough, W. D. Flanders, M. A. McGeehin, J. R. Lumpkin, Excess hospital admissions during the July 1995 heat wave in Chicago. *Am. J. Prev. Med.* **16**, 269–277 (1999).
34. C. J. Gronlund, A. Zanobetti, J. D. Schwartz, G. A. Wellenius, M. S. O'Neill, Heat, heat waves, and hospital admissions among the elderly in the United States, 1992–2006. *Environ. Health Perspect.* **122**, 1187–1192 (2014).
35. G. Mastrangelo, U. Fedeli, C. Visentin, G. Milan, E. Fadda, P. Spolaore, Pattern and determinants of hospitalization during heat waves: An ecologic study. *BMC Public Health* **7**, 200 (2007).
36. Office of Environmental Health Hazard Assessment (OEHHA), "Indicators of climate change in California" (2022); https://oehha.ca.gov/sites/default/files/media/humanhealthsection2022.pdf.
37. S. A. M. Khatana, R. M. Werner, P. W. Groeneveld, Association of extreme heat with all-cause mortality in the Contiguous US, 2008-2017. *JAMA Netw. Open* **5**, e2212957 (2022).
38. R. Xu, Q. Zhao, M. Coelho, P. H. N. Saldiva, M. J. Abramson, S. Li, Y. Guo, Socioeconomic inequality in vulnerability to all-cause and cause-specific hospitalisation associated with temperature variability: A time-series study in 1814 Brazilian cities. *Lancet Planet. Health* **4**, e566–e576 (2020).
39. U.S. Environmental Protection Agency (EPA), "Climate Change and Social Vulnerability in the United States: A Focus on Six Impacts" (Publication 430-R-21-003, EPA, 2021); https://www.epa.gov/system/files/documents/2021-09/climate-vulnerability_september-2021_508.pdf.
40. K. Chen, A. J. Newman, M. Huang, C. Coon, L. A. Darrow, M. J. Strickland, H. A. Holmes, Estimating heat-related exposures and urban heat island impacts: A case study for the 2012 Chicago heatwave. *Geohealth* **6**, e2021GH000535 (2022).
41. S. Whitman, G. Good, E. R. Donoghue, N. Benbow, W. Shou, S. Mou, Mortality in Chicago attributed to the July 1995 heat wave. *Am. J. Public Health* **87**, 1515–1518 (1997).
42. A. N. Kho, D. M. Hynes, S. Goel, A. E. Solomonides, R. Price, B. Hota, S. A. Sims, N. Bahroos, F. Angulo, W. E. Trick, E. Tarlov, F. D. Rachman, A. Hamilton, E. O. Kaleba, S. Badlani, S. L. Volchenboum, J. C. Silverstein, J. N. Tobin, M. A. Schwartz, D. Levine, J. B. Wong, R. H. Kennedy, J. A. Krishnan, D. O. Meltzer, J. M. Collins, T. Mazany, CAPriCORN Team, CAPriCORN: Chicago area patient-centered outcomes research network. *J. Am. Med. Inform. Assoc.* **21**, 607–611 (2014).
43. K. C. Young, D. A. Meza, B. Khuder, S. R. Rosenberg, G. Y. Liu, J. M. Kruser, P. A. Reyfman, R. Kalhan, Care fragmentation is associated with increased chronic obstructive pulmonary disease exacerbations in a U.S. urban care setting. *Am. J. Respir. Crit. Care Med.* **206**, 1044–1047 (2022).
44. U.S. Environmental Protection Agency, AirData: Air Quality Data Collected at Outdoor Monitors Across the US (accessed June 20, 2026).
45. Y. Benjamini, Y. Hochberg, Controlling the false discovery rate: A practical and powerful approach to multiple testing. *J. R. Stat. Soc. B Methodol.* **57**, 289–300 (1995).
46. P. M. Graffy, A. Sunderraj, M. A. Visa, C. H. Miller, B. W. Barrett, S. Rao, S. F. Camilleri, R. D. Harp, C. Li, A. Brenneman, J. Chan, A. Kho, N. Allen, D. E. Horton, Methodological approaches for measuring the association between heat exposure and health outcomes: A comprehensive global scoping review. *Geohealth* **8**, e2024GH001071 (2024).
47. W. L. Kenney, D. H. Craighead, L. M. Alexander, Heat waves, aging, and human cardiovascular health. *Med. Sci. Sports Exerc.* **46**, 1891–1899 (2014).
48. H. M. Choi, S. Heo, D. Foo, Y. Song, R. Stewart, J. Son, M. L. Bell, Temperature, crime, and violence: A systematic review and meta-analysis. *Environ. Health Perspect.* **132**, 106001 (2024).
49. C. A. Anderson, Temperature and aggression: Ubiquitous effects of heat on occurrence of human violence. *Psychol. Bull.* **106**, 74–96 (1989).
50. J. Lickiewicz, K. Piotrowicz, P. P. Hughes, M. Makara-Studzinska, Weather and aggressive behavior among patients in psychiatric hospitals-an exploratory study. *Int. J. Environ. Res. Public Health* **17**, 9121 (2020).
51. A. Nori-Sarma, S. Sun, Y. Sun, K. R. Spangler, R. Oblath, S. Galea, J. L. Gradus, G. A. Wellenius, Association between ambient heat and risk of emergency department visits for mental health among US adults, 2010 to 2019. *JAMA Psychiatry* **79**, 341–349 (2022).
52. L. E. Roberts, N. Bushover, C. A. Mehranbod, E. L. Eschliman, C. S. Fish, S. Zadey, C. N. Morrison, Extreme heat and firearm violence in New York city public housing: The mitigating role of air conditioning. *J. Urban Health* **102**, 344–351 (2025).
53. R. P. Larrick, T. A. Timmerman, A. M. Carton, J. Abrevaya, Temper, temperature, and temptation: Heat-related retaliation in baseball. *Psychol. Sci.* **22**, 423–428 (2011).
54. K. Bai, K. Li, L. Shao, X. Li, C. Liu, Z. Li, M. Ma, D. Han, Y. Sun, Z. Zheng, R. Li, N.-B. Chang, J. Guo,, LGHAP v2: A global gap-free aerosol optical depth and PM2.5 concentration dataset since 2000 derived via big Earth data analytics. *Earth Syst. Sci. Data* **16**, 2425–2448 (2024).
55. P. M. Graffy, B. W. Barrett, D. E. Horton, A. N. Kho, N. B. Allen, Critical temperature thresholds for identifying vulnerability to heat-related excess cardiovascular morbidity and mortality. *J. Am. Heart Assoc.* **15**, e046117 (2026).
56. P. M. Graffy, B. W. Barrett, D. E. Horton, N. B. Allen, A. N. Kho, Heat and hearts: An exposure-anchored computational phenotyping framework for assessing cardiovascular vulnerability during extreme heat. *J. Biomed. Inform.* **178**, 105029 (2026).
57. World Health Organization., *International Statistical Classification of Diseases and Related Health Problems* (World Health Organization, Geneva, ed. 10th revision, ed. 2, 2004).
58. Chicago Department of Public Health, Chicago Health and Health Systems Project, Serving Chicago's Underserved: Regional Health Systems Profiles (Chicago Department of Public Health, Chicago, IL, 2010).
59. M. Thornton, R. Shrestha, Y. Wei, P. Thornton, S.-C. Kao, Daymet: Daily surface weather data on a 1-km grid for North America, version 4 R1, *ORNL DAAC* (2022).
60. G. B. Anderson, M. L. Bell, Heat waves in the United States: Mortality risk during heat waves and effect modification by heat wave characteristics in 43 U.S. communities. *Environ. Health Perspect.* **119**, 210–218 (2011).
61. C. R. O'Lenick, S. E. Cleland, L. M. Neas, M. W. Turner, E. M. McInroe, K. L. Hill, A. J. Ghio, M. E. Rebuli, I. Jaspers, A. G. Rappold, Impact of heat on respiratory hospitalizations among older adults in 120 large U.S. urban areas. *Ann. Am. Thorac. Soc.* **22**, 367–377 (2025).
62. R. Marks, M. Rios-Vargas, Improvements to the 2020 Census Race and Hispanic Origin Question Designs, Data Processing, and Coding Procedures (U.S. Census Bureau, 2021).
63. A. Zanobetti, J. Schwartz, Temperature and mortality in nine US cities. *Epidemiology* **19**, 563–570 (2008).
64. A. Gasparrini, Y. Guo, M. Hashizume, E. Lavigne, A. Tobias, A. Zanobetti, J. D. Schwartz, M. Leone, P. Michelozzi, H. Kan, S. Tong, Y. Honda, H. Kim, B. G. Armstrong, Changes in susceptibility to heat during the summer: A multicountry analysis. *Am. J. Epidemiol.* **183**, 1027–1036 (2016).
65. A. M. Vicedo-Cabrera, N. Scovronick, F. Sera, D. Roye, R. Schneider, A. Tobias, C. Astrom, Y. Guo, Y. Honda, D. M. Hondula, R. Abrutzky, S. Tong, M. de Sousa Zanotti Stagliorio Coelho, P. H. N. Saldiva, E. Lavigne, P. M. Correa, N. V. Ortega, H. Kan, S. Osorio, J. Kysely, A. Urban, H. Orru, E. Indermitte, J. J. K. Jaakkola, N. Ryti, M. Pascal, A. Schneider, K. Katsouyanni, E. Samoli, F. Mayvaneh, A. Entezari, P. Goodman, A. Zeka, P. Michelozzi, F. de'Donato,

M. Hashizume, B. Alahmad, M. H. Diaz, C. De La Cruz Valencia, A. Overcenco, D. Houthuijs, C. Ameling, S. Rao, F. D. Ruscio, G. Carrasco-Escobar, X. Seposo, S. Silva, J. Madureira, I. H. Holobaca, S. Fratianni, F. Acquaotta, H. Kim, W. Lee, C. Iniguez, B. Forsberg, M. S. Ragettli, Y. L. L. Guo, B. Y. Chen, S. Li, B. Armstrong, A. Aleman, A. Zanobetti, J. Schwartz, T. N. Dang, D. V. Dung, N. Gillett, A. Haines, M. Mengel, V. Huber, A. Gasparrini, The burden of heat-related mortality attributable to recent human-induced climate change. *Nat. Clim. Change* **11**, 492–500 (2021).

66. S. Lee, A. M. Vicedo-Cabrera, Unveiling heat vulnerability of older adults: An assessment of emergency hospital admissions in Switzerland. *Int. J. Epidemiol.* **55**, dyag044 (2026).
67. R. E. Davis, W. M. Novicoff, The impact of heat waves on emergency department admissions in Charlottesville, Virginia, U.S.A. *Int. J. Environ. Res. Public Health* **15**, 1436 (2018).
68. A. Gasparrini, Distributed lag linear and non-linear models in R: The package dlnm. *J. Stat. Softw.* **43**, 1–20 (2011).

Acknowledgments

Funding: This work was supported by the American Heart Association (AHA) Predoctoral Fellowship 24PRE1193628 (awarded to P.M.G.) and Northwestern University's Buffett Institute for Global Affairs Defusing Disasters working group (awarded to D.E.H.). **Author contributions:** Conceptualization: A.N.K., H.J., P.M.G., B.W.B., D.E.H., and J.L.C. Methodology: A.N.K., H.J., P.M.G., B.W.B., J.L.C., and D.E.H. Software: A.N.K., H.J., P.M.G., and B.W.B. Validation: A.N.K., H.J., P.M.G., and B.W.B. Formal analysis: H.J. Investigation: H.J., P.M.G., and B.W.B. Data curation: P.M.G., B.W.B., and D.E.H. Visualization: H.J., P.M.G., and B.W.B. Writing—original draft: H.J. and P.G. Writing—review and editing: H.J., P.M.G., B.W.B., D.E.H., J.L.C., and A.N.K. Supervision: P.M.G., B.W.B., A.N.K., and D.E.H. Project administration: H.J., P.M.G., B.W.B., and D.E.H. Funding acquisition: D.E.H. Resources: A.N.K., H.J., P.M.G., B.W.B., and D.E.H. **Competing interests:** The authors declare that they have no competing interests. **Data, code, and materials availability:** All data and code needed to evaluate and reproduce the results in the paper are present in the paper and/or the Supplementary Materials. This study did not generate new materials. The findings reported in this study were enabled through a collaboration with CAPriCORN. CAPriCORN is a partnership between health care and research institutions that provides data through a federated harmonized common data model and works jointly with a Patient Community Advisory Committee, community-based organizations, and nonprofit organizations committed to enabling and delivering patient-centered clinical research and public health projects. We acknowledge CAPriCORN's partners, the Chicago Area Institutional Review Board (CHAIRb), which serves as the central IRB of record for CAPriCORN-supported research, and the Medical Research Analytics and Informatics Alliance, which serves as the network's honest data broker. The underlying data are not publicly available because of patient privacy and institutional data use agreements. The data can be provided by CAPriCORN pending scientific review and a completed data transfer agreement through CHAIRb. Requests for the data should be submitted to info@capricorncdrn.org.

Submitted 27 October 2025
Accepted 17 July 2026
Published 26 August 2026
10.1126/sciadv.aed3977